Soft Matter

Dynamic Article Links

Cite this: *Soft Matter*, 2012, **8**, 1301

www.rsc.org/softmatter

COMMUNICATION

Creasing instability of elastomer films

Shengqiang Cai,†[a] Dayong Chen,†[b] Zhigang Suo*[a] and Ryan C. Hayward*[b]

Received 28th September 2011, Accepted 1st December 2011
DOI: 10.1039/c2sm06844c

The creasing instability of elastomer films under compression is studied by a combination of experiment and numerical simulation. Experimentally, we attach a stress-free film on a much thicker and stiffer pre-stretched substrate. When the substrate is partially released, the film is uniaxially compressed, leading to formation of an array of creases beyond a critical strain. The profile of the folded surface is extracted using confocal fluorescence microscopy, yielding the depths, spacings, and shapes of creases. Numerically, the onset and development of creases are simulated by introducing appropriately sized defects into a finite-element mesh and allowing the surface of the film to self-contact. The measurements and simulations are found to be in excellent agreement.

When a soft elastic material—*e.g.* an elastomer or a gel—is compressed, the surface of the material is initially smooth, but then suddenly forms creases beyond a critical value of compression.[1–9] At each crease the surface folds into a region of self-contact with a sharp tip. As the force is increased, the crease deepens by enlarging the area of self-contact and submerging the tip further below the surface. Creases are often detrimental, *e.g.*, possibly initiating failure of tires[2] or modifying the behavior of cells cultured on soft substrates.[3] On the other hand, creases provide a flexible route to engineer switchable surfaces.[4] It is also intriguing to contemplate the role that this instability may play in the development and function of the brain and other soft tissues.

While creases are commonly observed, their scientific understanding is in a nascent stage. Previous attempts to quantitatively analyze experimental data on crease formation[2,5,6] have relied on Biot's linear instability analysis of the surface of a compressed elastomer,[10] which we refer to as a "wrinkling" instability. In the simplest context, both creasing and wrinkling represent a bifurcation from a state of homogeneous deformation. Wrinkles, wherein the surface of the material undulates sinusoidally but remains locally smooth, involve a deviation from the homogeneous state by a field of strain that is infinitesimal in amplitude, but finite in space. By contrast, creases are localized folds that represent a deviation from the homogeneous state by a field of strain that is finite in amplitude, but infinitesimal in space. Consequently, the critical condition for the onset of wrinkles can be determined by a classical linear perturbation analysis,[10] while the critical condition for the onset of creases cannot.

Recent impetus comes from the realization that, for homogeneous elastic materials under compression, creases set in before wrinkles.[11,12] For example, for neo-Hookean materials under plane-strain compression, nonlinear finite-element analyses[11–15] predict that formation of creases is energetically favored at a critical strain of $\varepsilon = 0.35$, substantially below the value of 0.46 for wrinkling.[10] Furthermore, Cao and Hutchinson carried out a post-bifurcation analysis of Biot's wrinkling instability and found that the wrinkled state is extremely unstable, meaning that it is highly defect sensitive and once formed is dynamically unstable to formation of a crease.[16] In practice, these results imply that: (i) the wrinkled state should never be an equilibrium solution for the surface of a compressed homogeneous material, and (ii) experimental observations on creases must be considered in the context of the nonlinear analysis, not the linear stability calculation. We note that both creases and Biot's wrinkling instability involve only a soft surface under compression, and should not be confused with the more extensively studied and better-understood case of wrinkling of a thin stiff film on a soft elastic foundation.[17–19] In the latter case, the near inextensibility of the much stiffer skin relative to the substrate leads to sinusoidal wrinkling at small compressive strains, with a wavelength that is well described by linear theory.

While the measured onset of creasing on a bent elastomer surface,[2] $\varepsilon = 0.35 \pm 0.07$, is in agreement with the nonlinear prediction, the large experimental uncertainty leaves doubt as to how closely the two values match. Further quantitative comparisons, for example on the spacings, shapes, or depths of folds, are completely lacking due to both modeling and experimental challenges. On the modeling side, the singularity of the creases and the necessity to break translational invariance have previously required introduction of a stiff skin whose thickness was gradually reduced in a limiting process,[11,12] prescription of a small crease through boundary conditions,[13] or application of a point force on the surface.[14] Besides the inconvenience of these methods, they have so far limited analysis mostly to initiation of a single crease, with few predictions available for fully formed folds. Experimentally, the study of creases on elastomeric blocks under simple compression is difficult since buckling or barreling instabilities usually occur at much lower strains. The solution to this problem has previously been to bend a rod or slab,[2,6,11,12] providing nearly plane-strain compression on the inner bend surface. However, in this geometry quantitative characterization beyond crease initiation is

[a]*School of Engineering and Applied Sciences, Kavli Institute, Harvard University, Cambridge, MA, 02138, USA. E-mail: suo@seas.harvard.edu*
[b]*Department of Polymer Science & Engineering, University of Massachusetts, Amherst, MA, 01003, USA. E-mail: rhayward@mail.pse.umass.edu*
† These authors contributed equally to this work.

complicated both by the inhomogeneous strain through the thickness of the specimens and the difficulty of measuring the spacing and shapes of the surface folds. Creases formed on swelling gel surfaces have received slightly more quantitative study,[4,5,9,20–22] but the challenges inherent to modeling swelling have made quantitative comparisons with theory difficult.

Here we study both the initiation and development of creases in homogeneously compressed elastomer films through a combination of simple experimental and numerical methods. This allows for detailed quantitative comparisons between experimental measurements and numerical predictions. We find that the onset, shape, and spacing of creases are very well described by calculations of the equilibrium elastic state for a neo-Hookean material with no adjustable parameters.

Fig. 1a illustrates the experimental approach, modified from a previous study of the snap-through instability of supported elastic membranes.[23] We apply a uniaxial tension to stretch a thick substrate from the original length L_0 to a length L, and then attach to the stretched substrate a stress-free film of thickness H that is much softer than the substrate. When the substrate is partially released to a length l, the film is subjected to a compressive strain $\varepsilon = 1 - (l/L)$. The film is in a state of uniaxial stress, because both the substrate and film are incompressible. The magnitude of the applied strain can be varied continuously, but is limited by $1 - (L_0/L)$, when the substrate is fully released. (We note that, while the current manuscript was under review, a similar experimental system was used to apply uniaxial compression to viscoelastic layers of microemulsions.[24])

The substrate and the film used in the experiment were polydimethylsiloxane (PDMS; Sylgard 184, Dow Corning) elastomers of different crosslink densities (15 : 1 and 40 : 1 base : crosslinker by weight, respectively), with a Young's modulus of 800 kPa for the substrate and 48 kPa for the film.[25,26] The marked difference in stiffness, as shown below, led to only small deviations from the idealized case of the model wherein the film/substrate interface remains planar. The film was bonded to the substrate by applying a thin adhesive layer of uncured 40 : 1 PDMS and subsequently crosslinking this layer prior to releasing the stretch of the substrate. While these materials display viscoelastic behavior, compression was performed slowly across the range of ε of interest (~30 min between each incremental application of a strain of ~0.01), and structures were measured only after allowing samples to equilibrate for at least 48 h, to ensure that the effects of viscous stresses were minimal.

Films with undeformed thicknesses of H = 23–147 μm were compressed by partially releasing the substrate, and observed *in situ* using an upright optical microscope. Beyond a certain level of strain, short creases formed in the vicinity of defects or scratches on the film surface, as shown in Fig. 1b, top left. At a higher level of strain, the creases extended laterally across the surface of the films, leading ultimately to an array of creases with fairly regular spacing (Fig. 1b, bottom right). This behavior complicates unambiguous identification of a critical strain. However, the smallest strain at which creases were found to propagate across the surface for any sample was $\varepsilon = 0.46$, providing an upper bound for the experimental value of the critical strain.

The creasing instability may also be affected by the PDMS/air surface energy γ, which, together with Young's modulus of the film E, yields a material-specific length[22] γ/E estimated as 0.4 μm based on a value of $\gamma = 20$ mN m^{-1}.[25] As long as the dimensionless number $\gamma/(EH)$ is sufficiently small, surface tension will have a negligible effect on the shape and spacing of creases. For the experiments described here, we estimate $\gamma/(EH)$ = 0.003–0.018, and thus we neglect the effect of surface energy in our calculations.

The onset of each crease is autonomous, occurring when any material point on the surface reaches a critical state of strain. Thus, the critical states of strain can be determined independent of the specific boundary conditions. For a neo-Hookean material, the conditions for the onset of creasing have been calculated under arbitrary states of strain.[13] The general solution shows that under uniaxial stress the critical strain is 0.44 for the onset of creasing, while the critical strain is 0.56 for the onset of wrinkles.[2]

To analyze both the onset and subsequent development of creases, we used the commercial finite-element software ABAQUS. The film is assumed to form a periodic array of creases, so that half of a period is selected as a calculation cell, as illustrated in the inset of Fig. 2, with W being the period in the undeformed state. A symmetric boundary condition is applied on the right boundary of the cell, while a uniform horizontal displacement is prescribed on the left boundary. The top surface of the film is traction free. The substrate is taken to be much stiffer than the film, so that the bottom of the cell remains flat. The shear stress on the bottom surface is assumed to be negligible. Since a crease will emerge wherever the strain first exceeds the critical value, only a small perturbation is necessary to break translational invariance and specify the position of the crease. The small perturbation is introduced by placing in the finite-element mesh a defect—a quarter of a circle of a small radius; see the inset of Fig. 2. To eliminate the

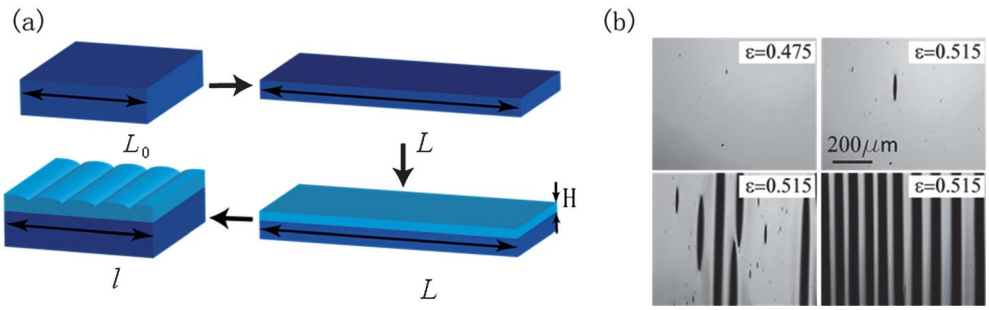

Fig. 1 (a) A schematic of the experiment by which an elastomeric film of initial thickness H is placed under uniaxial compressive strain by partial release of a much thicker and stiffer elastomeric substrate. (b) Reflectance optical micrographs show the nucleation and growth of creases for a film of $H = 63$ μm. At $\varepsilon = 0.475$, short folds formed in the vicinity of defects but did not propagate, while at $\varepsilon = 0.515$, lateral growth of creases (top right to bottom left) eventually led to formation of a parallel array of folds (bottom right).

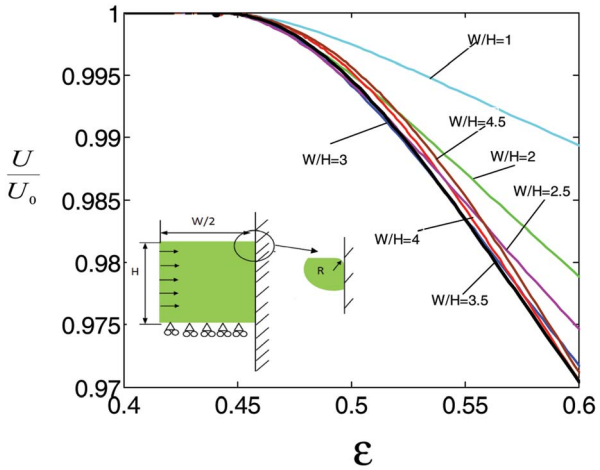

Fig. 2 The normalized elastic energy of the creased state plotted as a function of the uniaxial compressive strain. The creases are assumed to form a periodic array defined by the aspect ratio of the simulation cell (the inset illustrates half of the periodic cell). While the dependence on periodicity is rather weak, the elastic energy is nearly minimized by a value of $W/H \approx 3.5$ across the range of strains studied experimentally.

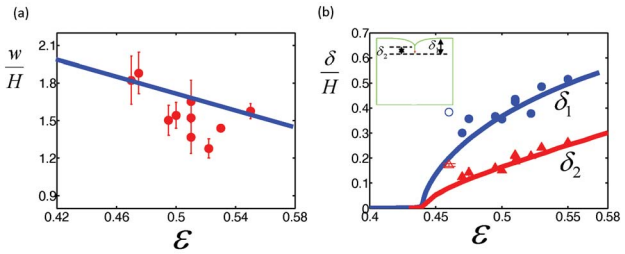

Fig. 3 (a) The equilibrium spacing of creases as a function of the compressive strain. The solid line is predicted by the calculation, and the symbols are experimental measurements, with error bars representing the standard deviation of average fold spacings measured at different positions on the sample surface. (b) The equilibrium depth of crease as a function of the compressive strain. The solid curves are predicted by the calculation, and symbols are experimental measurements. The open entries at a strain of 0.46 correspond to an isolated crease, while the filled symbols at higher strains are measured for parallel arrays of creases.

effect of the size of the defect, the defect is made much smaller than the thickness of the film H. To resolve the field close to the tip of the crease, the defect is made much larger than the size of the finite elements around the defect. The surface of the film is allowed to fold and self-contact. We also varied the size and shape of the defect and did not find any effect on the results we report, provided that the size was sufficiently large compared to the mesh and sufficiently small compared to the block thickness.

Fig. 2 shows the calculated elastic energy of the cell in the creased state, U, normalized by the elastic energy of the uniformly compressed cell in the absence of the crease, U_0, as a function of the applied strain ε, for several values of W/H. When $\varepsilon < 0.44$, for all the values of W/H, the defect has a negligible influence on the elastic energy. When $\varepsilon > 0.44$, the defect will induce a crease and reduce the elastic energy of the elastomer. The critical strain 0.44 matches precisely the result previously obtained with a different numerical approach,[13] and is in excellent agreement with the experimentally observed upper bound of 0.46 as described above.

The elastic energy is nearly minimized across the full range of applied strains covered by our experiment ($\varepsilon = 0.46$–0.55) for a ratio of $W/H \approx 3.5$. Since the spacing between creases in the deformed state is $w = (1 - \varepsilon)W$, we predict that the equilibrium spacing between creases should be $w/H \approx 3.5(1 - \varepsilon)$. This prediction is plotted in Fig. 3a, together with the experimental measurements. The magnitudes of the predicted and observed wavelengths are in good agreement, though the scatter in the experimental data precludes a more detailed comparison of the dependence on strain. While it has long been appreciated that the characteristic spacing between creases must scale as the film thickness,[1] as this is the only relevant length scale in the problem, our results represent the first prediction of the pre-factor in this scaling relationship, as well as the first measurement of crease spacings for elastomers. Notably, experiments revealed a well-defined characteristic spacing of creases, but not perfectly regular packing (Fig. 1b), and once a parallel array had formed, further compression led to only "affine" changes, never to annihilation or appearance of new creases. These observations are consistent with the relatively weak dependence of elastic energy on aspect ratio shown in Fig. 2, and also indicate that creases are not able to fully equilibrate, thus yielding sensitivity of the observed spacing to sample history.

Fig. 3b shows the calculated distance from the uppermost point on the surface to the bottom of the crease tip δ_1 and the depth of the self-contacting region δ_2. Experimentally, both the film and adhesive layer were doped with a small amount of fluorescent monomer (fluorescein acrylate) that labels both layers but also partitions preferentially to the film/air interface. As shown in Fig. 4, this partition allowed unambiguous determination of the entire surface profile in the creased state by laser scanning confocal microscopy (of films immersed in a refractive index matched fluid of 72% by weight glycerol and 28% water)—including the self-contacting region of the surface and the film/substrate interface—details that have previously been unavailable from experiments on bent slabs or rods.[2,6,11,12] Fig. 3b shows close correspondence between the measured and predicted equilibrium values of δ_1 and δ_2, for all data points except those at $\varepsilon = 0.46$ (open symbols). This value is just slightly above the critical strain, and thus only isolated creases were formed, which have different shapes than those in an array.

Fig. 4 shows the calculated surface profiles overlaid on the experimental data for three values of strain, with only an isotropic scaling factor proportional to $1/H$ applied to each refractive-index-corrected cross-section. It can be seen that the calculations not only capture the depth and spacing of the creases, but also accurately describe the shape of the free surface. In Fig. 4c it can be seen that the film/substrate interface did not remain entirely planar, but the amplitude of corrugations was less than 3% of the film thickness at the highest applied strain of $\varepsilon = 0.55$. Thus, while the experimental geometry does not exactly match that of the simulation, any resulting deviations will be minor.

We emphasize that, apart from the choice of a neo-Hookean strain energy function used to describe the elastomeric block, there are no adjustable parameters in our model. Thus, the agreement between calculations and experiments presented in Fig. 3 and 4 is remarkably good.

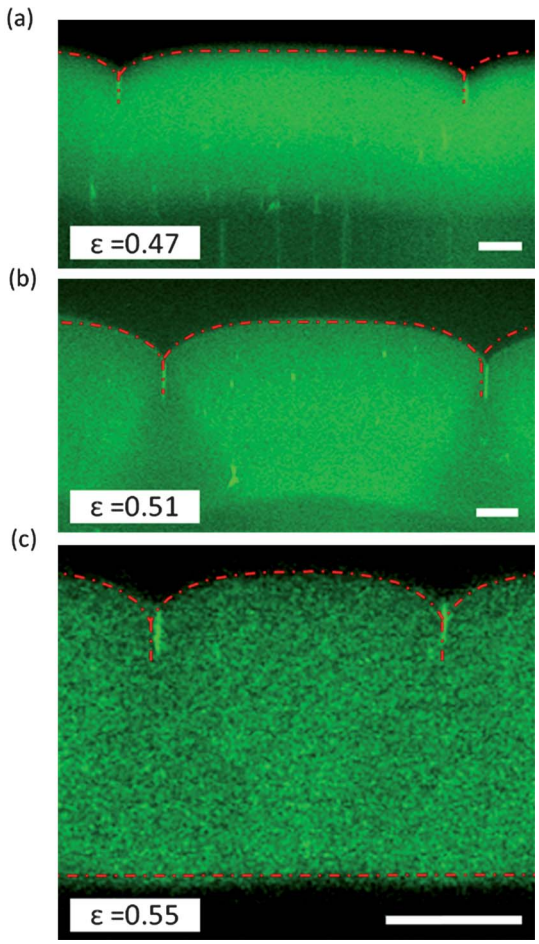

Fig. 4 Comparisons between calculated surface profiles (red dotted lines) and experimental cross-sections determined by confocal microscopy (green images), for elastomer surfaces in the creased state at three levels of strain. Initial film thicknesses H were (a) 93 μm, (b) 91 μm and (c) 23 μm (scale bars represent 20 μm). For the thinnest film in (c), it is also possible to observe the film/substrate interface.

In summary, we have introduced an experimental approach to place thin elastomeric films under homogeneous compression, leading to arrays of creases that can be characterized in detail, along with a numerical method that provides straightforward calculations of equilibrium crease structures. The excellent quantitative agreement obtained between the measured and calculated depths, spacings, and shapes of creases indicates that the onset and development of folds on the surface of a compressed elastomer are very well described by a simple nonlinear finite element analysis, so long as an appropriately sized defect is introduced to seed formation of a finite amplitude fold. We anticipate that these will represent enabling experimental and numerical tools for future quantitative studies of crease nucleation, growth, and hysteresis, and furthermore will allow for engineering of thin elastomeric films with switchable micro-patterns and surface properties.

This study was funded by Multidisciplinary University Research Initiative (MURI) (W911NF-09-1-0476), and Materials Research Science and Engineering Center (MRSEC) at Harvard University. DC and RH were supported by the National Science Foundation through grant DMR-0747756, with additional funding from the MRSEC on Polymers at UMass (DMR-0820506) and a 3M Nontenured Faculty Grant.

References

1 T. Tanaka, S.-T. Sun, Y. Hirokawa, S. Katayama, J. Kucera, Y. Hirose and T. Amiya, *Nature*, 1987, **325**, 796.
2 A. N. Gent and I. S. Cho, *Rubber Chem. Technol.*, 1999, **72**, 253.
3 K. Saha, J. Kim, E. Irwin, J. Yoon, F. Momin, V. Trujillo, D. V. Schaffer, K. E. Healy and R. C. Hayward, *Biophys. J.*, 2010, **99**, 94.
4 J. W. Kim, J. W. Yoon and R. C. Hayward, *Nat. Mater.*, 2010, **9**, 159.
5 V. Trujillo, J. Kim and R. C. Hayward, *Soft Matter*, 2008, **4**, 564.
6 A. Ghatak and A. L. Das, *Phys. Rev. Lett.*, 2007, **99**, 076101.
7 P. M. Reis, F. Corson, A. Boudaoud and B. Roman, *Phys. Rev. Lett.*, 2009, **103**, 045501.
8 Q. M. Wang, L. Zhang and X. H. Zhao, *Phys. Rev. Lett.*, 2011, **106**, 118301.
9 J. Dervaux and M. Ben Amar, *J. Mech. Phys. Solids*, 2011, **59**, 538.
10 M. A. Biot, *Appl. Sci. Res., Sect. A*, 1963, **12**, 168.
11 E. B. Hohlfeld, PhD thesis, Harvard University, 2008.
12 E. Hohlfeld and L. Mahadevan, *Phys. Rev. Lett.*, 2011, **106**, 105702.
13 W. Hong, X. H. Zhao and Z. G. Suo, *Appl. Phys. Lett.*, 2009, **95**, 111901.
14 W. H. Wong, T. F. Guo, Y. W. Zhang and L. Cheng, *Soft Matter*, 2010, **6**, 5743.
15 S. Q. Cai, K. Bertoldi, H. M. Wang and Z. G. Suo, *Soft Matter*, 2010, **6**, 5770.
16 Y. Cao and J. W. Hutchinson, *Proc. R. Soc. A*, 2012, **468**, 94.
17 S. Q. Cai, D. Breid, A. J. Crosby, Z. G. Suo and J. W. Hutchinson, *J. Mech. Phys. Solids*, 2011, **59**, 1094–1114.
18 C. N. Bowden, S. Brittain, A. G. Evans, J. W. Hutchinson and G. M. Whitesides, *Nature*, 1998, **393**, 146–149.
19 Z. Y. Huang, W. Hong and Z. G. Suo, *J. Mech. Phys. Solids*, 2005, **53**, 2101–2118.
20 M. Guvendiren, J. A. Burdick and S. Yang, *Soft Matter*, 2010, **6**, 5795.
21 M. K. Kang and R. Huang, *J. Mech. Phys. Solids*, 2010, **58**, 1582.
22 J. Yoon, J. Kim and R. C. Hayward, *Soft Matter*, 2010, **6**, 5807.
23 D. P. Holmes and A. J. Crosby, *Adv. Mater*, 2007, **19**, 3589.
24 S. Mora, M. Abkarian, H. Tabuteau and Y. Pomeau, *Soft Matter*, 2011, **7**, 10612.
25 O. D. Gordan, B. N. J. Persson, C. M. Cesa, D. Mayer, B. Hoffmann, S. Dieluweit and R. Merkel, *Langmuir*, 2008, **24**, 6636.
26 E. A. Wilder, S. Guo, S. L. Gibson, M. J. Fasolka and C. M. Stafford, *Macromolecules*, 2006, **39**, 4138–4143.